Available online at www.sciencedirect.com
SCIENCE DIRECT
ELSEVIER
Colloids and Surfaces A: Physicochem. Eng. Aspects 272 (2006) 32–36
COLLOIDS AND SURFACES A
www.elsevier.com/locate/colsurfa

Evaluation of the zinox and zeolite materials as adsorbents to remove H_2S from natural gas

D.M.A. Melo [a,*], J.R. de Souza [b], M.A.F. Melo [b], A.E. Martinelli [a], G.H.B. Cachima [a], J.D. Cunha [a]

[a] *Laboratório de Análise Térmica e Materiais, Departamento de Química, Universidade Federal do Rio Grande do Norte, CP: 1662, CEP: 59072-970, Natal, RN, Brazil*
[b] *Departamento de Engenharia Química, Universidade Federal do Rio Grande do Norte, CP: 1662, Natal, RN, Brazil*

Received 31 May 2005; received in revised form 29 June 2005; accepted 8 July 2005
Available online 18 August 2005

Abstract

Mesoporous materials can be generally used as adsorbents to remove impurities from gases. During the past few years, H_2S has been removed from natural gas using materials such as dolomite, zeolites, and industrial compounds, which can be widely used by oil and natural gas companies. The present study focused on the use of Zeolite 13X and Zinox 380 as H_2S adsorbent at 25 °C. They were characterized by chemical analyses (X-ray fluorescence and atomic absorption), X-ray diffraction, particle size distribution analyses and FT Infrared spectroscopy. Adsorption reactions were carried out using proposed models. The results revealed that both materials studied could be used as H_2S adsorbents in natural gas exceeding the capabilities of industrial compounds.

Keywords: Mesoporous materials; Natural gas; Zeolite

1. Introduction

The composition of fossil fuels includes sulfur compounds as its major contaminants. The main examples include hydrogen sulfide (H_2S), mercaptanes (R-SH) and other organic sulfides such as RS, RS_2 or R_2S (where R represents either an aryl or alkyl group). Sulfur is released to the atmosphere in the form of SO_2 as a result of the combustion of gaseous fuels. SO_2 can be oxidized to water-soluble SO_3 thus producing the so-called acid rain, which is highly hazardous to the environment and health. The H_2S present in natural gas is one of the major causes of corrosion in ducts and transport lines; in addition to being extremely toxic and lethal even in concentrations as low as a few ppm.

Several studies [1–12] have addressed the removal of sulfurous compounds using adsorbent materials such as molecular sieves and polymeric adsorbents. These materials depict a series of valuable properties and characteristics to adsorption processes, including high specific area, porous bulk structure, uniform distribution of pores, good resistance to high temperatures and improved selectivity. In this context, the present study aimed at evaluating the characteristics and performance of Zinox 380 (88% ZnO) and Zeolite 13X, particularly for future use by PETROBRAS Cia. in its Natural Gas Processing Plant located in Guamaré, Northern Brazil. The new desulphurization process is based on the reaction of the sulfurous compounds present in natural gas with a solid material encountered in fixed bed reactors. As the bed is saturated and no longer reacts with sulfur, the resulting inert solid material can be safely discarded.

2. Experimental

Zeolite 13X was supplied by GRACE Corporation whereas zinc oxide (Zinox 380) was purchased from Oxiteno Brazil. These materials were chemically characterized by

* Corresponding author. Tel.: +55 84 3211 9241; fax: +55 84 3211 9241.
E-mail address: dmelo@matrix.com.br (D.M.A. Melo).

0927-7757/$ – see front matter © 2005 Elsevier B.V. All rights reserved.
doi:10.1016/j.colsurfa.2005.07.005

atomic absorption using a VARIAN equipment and X-ray fluorescence in a SHIMADZU analyzer. Thermogravimetric curves and their corresponding derivatives were obtained in a Perkin-Elmer TGA-7 thermal balance under N_2 flowing at 50 mL/min using 20 mg samples. The heating rate was set to 10 °C/min and the temperature range from 40 to 900 °C was monitored. Particle size distributions were determined according to ABNT guidelines down to 100 meshes. Powder X-ray diffraction patterns were obtained using a SIEMENS apparatus. Cu Kα radiation was used to scan the angular range $5 \leq 2\theta \leq 75^\circ$ at 1°/min. FT-IR patterns in the 4000 to 500 cm^{-1} range were also obtained using a BOMEM set-up to scan samples of the material dispersed into KBr pellets. The specific area of the powders was estimated using MICROMERITICS ASAP 2000 BET equipment. Prior to specific area measurements, the samples were maintained under vacuum for 3 h at 200 °C in order to remove adsorbed impurities. Nitrogen at 77 K was used as adsorbent gas for such analyses.

The adsorption column used in the experiments was 3.175 mm in diameter and 40 mm in height. It was made of 316 stainless steel to minimize effects related to corrosion by H_2S. The system was fed with a synthetic mixture of CH_4/H_2S at 100 ppm (White Martins Cia). The inlet pressures were adjusted and the outlet flow was controlled using a Hooke micrometric valve. The temperature of the column was maintained constant using a thermostatic bath from Automatic Systems Laboratories. The flow of gas to the column was monitored using a digital ADM 1000 flow meter by Humonics. Prior to adsorption runs, the bed was heated up and purged with N_2 4.6 (99.996 %) during 1 h. Natural gas flowed into the adsorption column at 30mL/min. The pressure was then adjusted to 5.0 kgf/cm^2 and temperature to 25 or 76 °C.

Gas chromatography was carried out using a Varian CP-3800 set-up equipped with a flame ionization detector (FID), a thermal conductivity detector (TCD) and a pulsed flame photometric detector (PFPD). The concentration of H_2S on the bed was monitored by the PFPD. A Varian CP Sil 5 CB chromatographic column was used to isolate the sulfurous compounds from natural gas. Rupture curves were obtained from mass balance aiming at establishing the volume of gas adsorbed by the solid. To that end, the following equations were used.

Mass of incoming adsorbate up to time t:

$$M_{in} = QC_0 \int_0^t dt = QC_0 t \quad (1)$$

Mass of outcoming adsorbate up to time t:

$$M_{out} = Q \int_0^t C dt = QC_0 \int_0^t \frac{C}{C_0} dt \quad (2)$$

Hence, the adsorbed mass can be expressed as:

$$M_{ads} = M_{in} - M_{out} \quad (3)$$

alternatively rewritten as:

$$M_{ads} = QC_0 t - QC_0 \int_0^t \frac{C}{C_0} dt \quad (4)$$

or:

$$M_{ads} = QC_0 \int_0^t \left(1 - \frac{C}{C_0}\right) dt \quad (5)$$

where Q is the flow (mL/min), C_o, the initial concentration of H_2S (ppm), C, the concentration of outcoming H_2S (ppm) and M_{ads} adsorbed mass (mg/g).

Some theoretical models were used to correlate the adsorption equilibrium data, including Langmuir's model and one of its extensions as well as Freundlich's, Langmuir–Freundlich's and Toth's models. The parameters used in these models were adjusted by the computer program Statistica 5.0. In addition, the Hooke-Jeeves and quasi-Newton methods were employed to determine the correlation coefficients. The Simplex method was used to recalculate the coefficients whenever the Hooke-Jeeves approach attributed unusually low values to those parameters.

3. Results and discussion

The chemical composition of Zeolite 13X was established as 1 Na_2O: Al_2O_3: 2.8 ± 0.2 SiO_2: X H_2O, where X depends on the dryness or activation of the material. The average pore size of zeolite was 10 Å. The composition of commercially available Zinox 380 is 87.1 wt.% ZnO, 0.2 wt.% Na_2O and 22.7% CaO. The X-ray diffraction patterns corresponding to Zinox 380 and Zeolite 13X are shown in Fig. 1. Zeolite 13X revealed diffraction peaks typical of zeolites with the faujasite structure (FAU) [13–15].

Results from thermogravimetric analyses performed in Zinox 380 Fig. 2 shows 1.5 wt.% loss from 40 to 230 °C

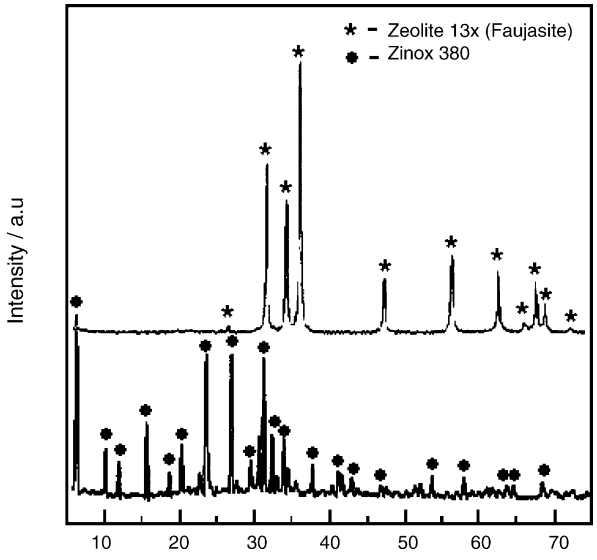

Fig. 1. X-ray diffraction pattern of Zinox 380 and Zeolite 13X.

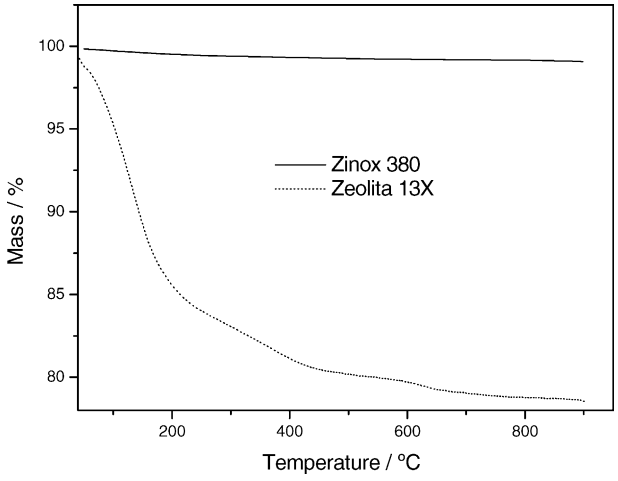

Fig. 2. TG curves of Zinox 380 and Zeolite 13X.

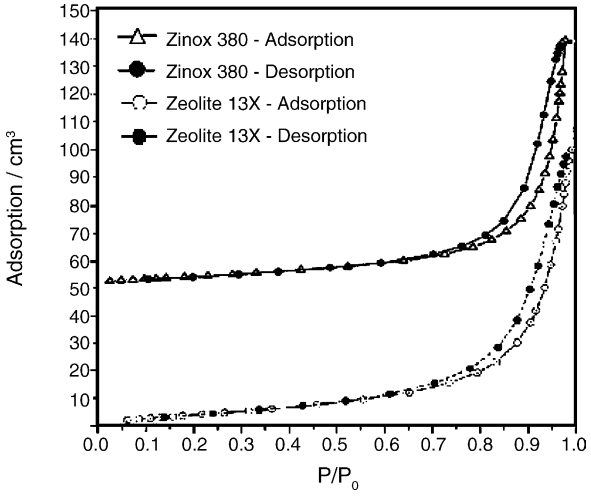

Fig. 4. Nitrogen adsorption isotherms of Zinox 380 and Zeolite 13X.

corresponding to hydration water. This material is stable up to 850 °C, at which temperature a stable oxide is formed. The thermal behavior of Zeolite 13X. Fig. 2 shows three different stages of weight loss corresponding to hydration water, zeolitic water and dehydroxylation. The infrared spectra corresponding to Zinox 380 is shown in Fig. 3. Stretching bands corresponding to ν_{OH} from hydration water were observed between 3000 and 3500 cm^{-1} along with a band around 1400 cm^{-1} characteristic of calcium oxide. Finally, bands in the vicinity of 1100 cm^{-1}, characteristic of the TO_4 (T = Zn) interaction and 1600 cm^{-1}, characteristic of hydroxyls were also observed. The infrared profile of zeolite Fig. 3 shows characteristic bands at 450, 550, 750 and 1100 cm^{-1} corresponding to SiO_4 and AlO_2 tetrahedra. Bands around 3500 cm^{-1} were also observed and attributed to hydroxyls.

The nitrogen adsorption–desorption isotherms illustrated in Fig. 4 depict type IV characteristic behavior. The point where $P/P_o = 1$ corresponds to complete pore filling up. The hysteresis observed from all samples corresponded to capillary condensation. This situation takes place as the equilibrium vapor pressure over a concave liquid meniscus is lower than the saturation vapor pressure (P_o) at the same temperature. As a consequence, vapor typically condenses in the mesopores of a solid whenever the relative pressure is lower than unit. The specific surface area of Zinox and Zeolite 13X were 34.54 m^2/g and 16.15 m^2/g, respectively. These values were in good agreement with the estimated area of a few micropores for both adsorbent samples. Such feature is ideal to oxides and zeolites and indicates that the material is adequate to be used as adsorbent to natural gas.

The isotherms and rupture plots for each adsorbent tested are shown in Figs. 5–8. Adsorption equilibrium experiments were carried out at 25 and 76 °C. These values were selected to simulate, respectively, ambient and operational temperatures typical of PETROBRAS unit in Guamaré-RN/Brazil. The equilibrium for the adsorption of H_2S molecules onto the surface of adsorbents granted information with respect to the adsorption capacity, saturation time, isotherm type, surface properties and adsorbent–adsorbate interaction. Experimental data were correlated to models represented by Eqs. (1)–(5). Hooke-Jeeves and/or Simplex algorithms were used together with the quasi-Newton one in order to calculate the coefficients corresponding to each model. During the first 15 min, the slope of the plot for Zinox was higher at

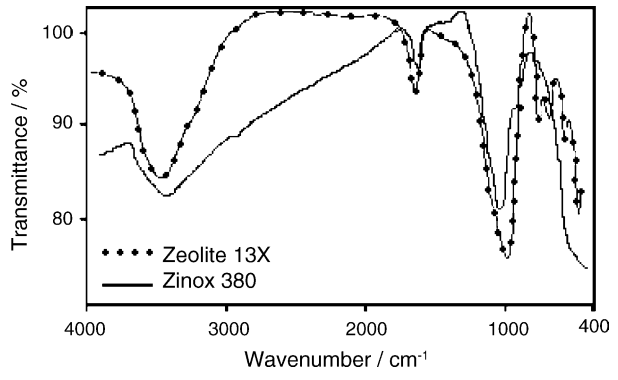

Fig. 3. Infrared spectra of Zinox 380 and Zeolite 13X.

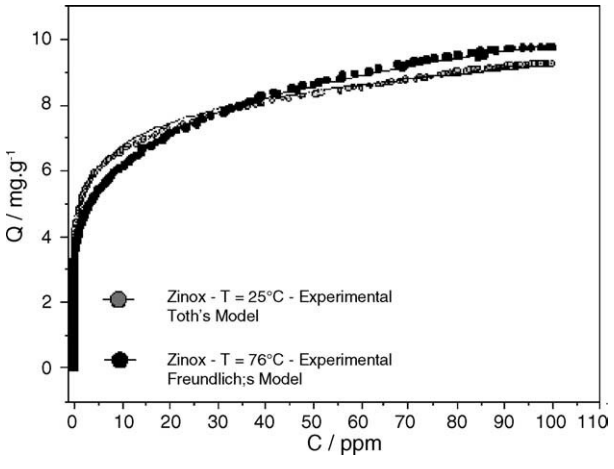

Fig. 5. Adsorption isotherms for Zinox 380 at 25 °C and Zinox 380 at 76 °C.

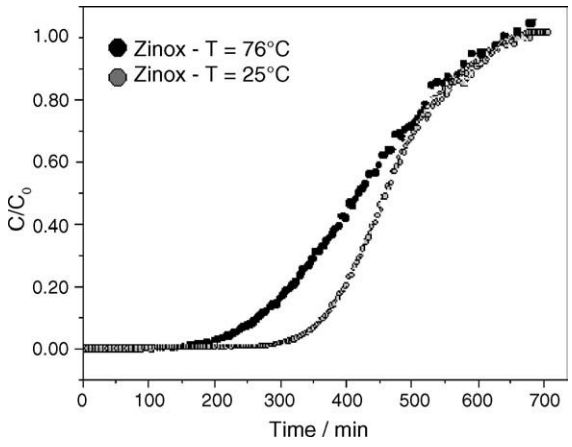

Fig. 6. Rupture curves for Zinox 380 at 25 °C and at Zinox 380 at 76 °C.

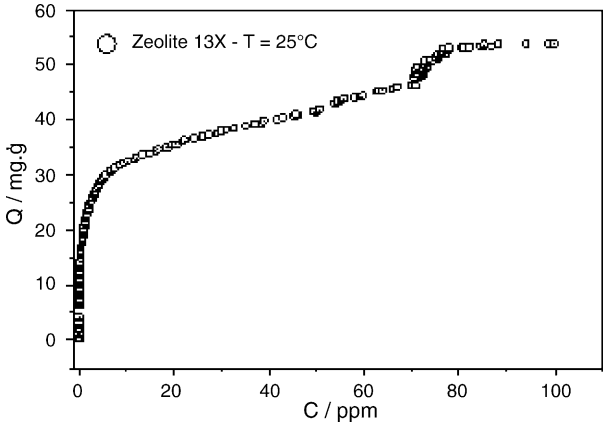

Fig. 7. Adsorption isotherm for Zeolite 13X at 25 °C.

25 °C (Fig. 5) than at 76 °C (Fig. 5), suggesting that the interaction between adsorbent and adsorbate was stronger for relatively lower temperatures. The isotherms illustrated in Fig. 5 show rapid adsorption at concentrations ranging from 0 to 10 ppm and from 20 to 90 ppm. After that, moderate adsorption was observed up to complete pore filling, which occurred at concentrations of 9.5 mg H_2S/g at 25 °C and 6.0 mg H_2S/g at 76 °C. The parameters obtained or the correlations of the experimental data with theoretical models are listed in Table 1. A good correlation could be observed using Toth's model.

The rupture curve for Zinox at 25 °C (Fig. 6) remained constant during the first 300 min. The concentration in the entrance of the bed was 100 ppm, and a reduction from this

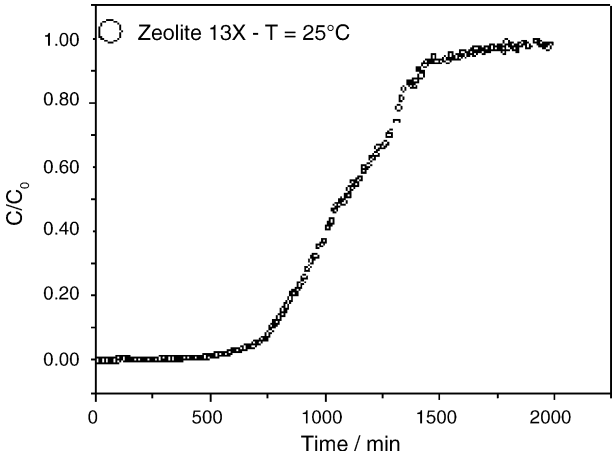

Fig. 8. Rupture curve for Zeolite 13X at 25 °C.

value to zero could be observed in that time interval. Next, the concentration in the exit of the bed increased up to saturation ($C/C_o = 1$). On the other hand, the rupture curve at 76 °C (Fig. 6) revealed that C/C_o remained constant only during the first 150 min for Zinox 380 and the final concentration was the same as that shown in Fig. 6. Table 2 shows the parameters for the models of the desulphurization isotherms for Zinox 380 at 76 °C.

The isotherm represented in Fig. 7, corresponding to Zeolite 13X, showed better results for the desulphurization of natural gas. The maximum adsorption capacity at 25 °C was 53 mg H_2S/g of adsorbent. Once again, Toth's model best fitted the experimental results, as confirmed by the parameters listed in Table 3. The rupture curve is shown in Fig. 8 and corresponded to long saturation times (approximately 36 h).

The materials characterized herein depicted the performance required by PETROBRAS to adsorb H_2S from natural gas. Nevertheless, isotherms acquired under the same temperature (25 °C) revealed better adsorption of H_2S by Zeolite 13X. This is probably related to the distinct nature of the porosity for Zinox 380 (micropores) and zeolite (mesoporos). For Zinox 380, increasing the temperature decreased both the absorbed volume of H_2S and the saturation time (16.67 h at 25 °C and 13.36 h at 76 °C), suggesting that the TSA method can be used in the regeneration of the bed. Eqs. (1)–(5) satisfactory establish correlations between equilibrium data. In most cases, Toth's and Freundlich's were adequate to fit the desulphurization process of natural gas, as suggested by the corresponding values of the correlation

Table 1
Parameters of the models for the desulphurization isotherms of Zinox 380 at 25 °C

Models						
	Langmuir	Freundlich	LangFre	LangFre3P	LangExtend	Toth
q_s	8.381	–	23.294	18.83	9.685	39.748
b	2.594	4.601	0.2495	0.007	850686.6	549.02×10^5
c	–	6.554	0.2089	0.229	890.116	0.088
R	0.923	0.979	0.979	0.979	0.967	0.979

Table 2
Parameters for the models of the desulphurization isotherms for Zinox 380 at 76 °C

Models						
	Langmuir	Freundlich	LangFre	LangFre3P[a]	LangExtend	Toth
q_s	5.666	–	31.141	13.212	7.178	122.3956
b	0.391	2.444	0.084	0.0052	540814.2	253680582
c	–	5.029	0.227	0.2862	1707.99	0.0644
R	0.936	0.989	0.989	0.987	0.976	0.988

[a] Simplex method.

Table 3
Parameters of the models for the desulphurization isotherms of Zeolite 13X at 25 °C

MODELS						
	Langmuir	Freundlich	LangFre	LangFre3P	LangExtend	Toth
q_s	37.540		–	45.221	–	48.782
b	1.0191	17.764	–	0.5166	–	3.647
c	–	4.339	–	0.604	–	0.452
R	0.973	0.968	–	0.983	–	0.984

coefficients, R, listed in Tables 1–3. Best fitting was achieved by the Langmuir–Freundlich 3P model at 25 °C and Toth's model at 76 °C. Strong indications of physical adsorption were gathered for both adsorbent materials tested.

4. Conclusions

Both Zeolite 13X and Zinox 380 can be used as adsorbents to remove H_2S from natural gas. Zeolite 13X revealed better adsorption of H_2S than Zinox at 25 °C. These results also showed that the distinct nature of the porosity for Zinox 380 (micropores) and zeolite (mesoporos) as a function of temperature determined longer saturation times for Zeolite 13X (36.5 h at 25 °C). In most cases, Toth's and Freundlich's models were adequate to fit the desulphurization process of natural gas, as suggested by the corresponding values of the correlation coefficients, R. Strong indications of physical adsorption were also observed for both adsorbent materials tested.

Acknowledgement

This work was supported by Conselho Nacional de Pesquisa e Desenvolvimento (CNPq), Project CT-PETRO 2002.

References

[1] T. Kopac, Chem. Eng. Process. 38 (1) (1999) 45.
[2] D.M. Ruthven, Zeolite as selective adsorbents, Chem. Eng. Prog., 1988.
[3] S.V. Gollakota, D. Chriswell, Ind. Eng. Chem. Res. 27 (1) (1988) 139;
A. Al-Shawabkeh, H. Matsuda, M. Hasatani, AIChE J. 43 (1) (1997) 173.
[4] J. Tantet, M. Eic, R. Desal, Gas Sep. Purif. 9 (3) (1995) 213.
[5] T.J. Bandosz, Carbon 37 (1999) 483.
[6] M.P. Cal, B.W. Stricker, A.A. Lizzio, Carbon 38 (2000) 1757.
[7] M.P. Cal, B.W. Stricker, A.A. Lizzio, S.K. Gangwal, Carbon 38 (2000) 1767.
[8] H.L. Chiang, J.H. Tsai, D.H. Chang, F.T. Jeng, Chemosphere 41 (2000) 1227.
[9] E.S. Kikkinides, R.T. Young, Ind. Eng. Chem. Res 30 (1991) 1981.
[10] E.S. Kikkinides, R.T Yang, Ind. Eng. Chem. Res. 32 (10) (1993) 2365.
[11] M. Mello, M. Eic., Porous Mater. Environ. Friendly Process 125 (1999) 657.
[12] H. Wakita, Y. Tachibana, M. Hosaka, Micropor. Mesopor. Mater. 46 (2001) 237.
[13] M.M.J. Treacy, J.B. Higgins (Eds.), Collection of Simulated XRD Powder Patterns for Zeolites, 4th ed., International Zeolite Association, Elsevier, 2001.
[14] W.M. Meier, D.H. Olson, C. Baerlocher, Atlas of Zeolite Structure Types, Elsevier, New York, 1996.
[15] H. McMurdie, Powder Diffraction Data 1 (1986) 76.